REVISITING $B_{20}H_{16}$ BY MEANS OF A JOINT COMPUTATIONAL/EXPERIMENTAL NMR APPROACH

Drahomír Hnyk[a1,*], Josef Holub[a2], Tomáš Jelínek[b], Jan Macháček[a3] and Michael G. S. Londesborough[a4,*]

[a] *Institute of Inorganic Chemistry, Academy of Science of the Czech Republic, v.v.i., 250 68 Husinec-Řež, Czech Republic; e-mail: [1] hnyk@iic.cas.cz, [2] holub@iic.cas.cz, [3] jmach@iic.cas.cz, [4] michaell@iic.cas.cz*

[b] *Katchem Ltd., 250 68 Husinec-Řež, Czech Republic; e-mail: t.jelinek@seznam.cz*

Received June 11, 2010
Accepted September 13, 2010
Published online November 9, 2010

Dedicated to Professor Bohumil Štíbr on the occasion of his 70th birthday as our gratitude to his achievements in boron cluster chemistry.

A new synthesis of the fused macropolyhedral boron cluster $B_{20}H_{16}$ is described and its molecular structure in solution discussed, based on multi-nuclear NMR spectra, including *COSY* measurements, in relation to its previously elucidated solid-state structure. To verify the conclusions from the NMR study, experimentally determined chemical shifts are compared with calculated values at the GIAO-B3LYP level with a TZP basis set by Huzinaga. There is a very good agreement between the experimental and computed $\delta(^{11}B)$ values, suggesting that the MP2/6-31G* internal coordinates are a reasonable representation of the molecular geometry of this twenty-vertex cluster in solution that is essentially the same as its solid-state structure. A computational analysis of the FMO orbitals of $B_{20}H_{16}$, in particular of the LUMO, reveals that the four naked boron atoms, common for two shared icosahedral subclusters, are the reactive sites of this D_{2d}-symmetrical molecule.

Keywords: Boron; Ab initio calculations; NMR spectroscopy; Clusters.

The icosahedron is the most symmetrical way to arrange twelve atoms into a polyhedral cluster and is the quintessential structural motif in boron hydride cluster chemistry, classically represented by the [*closo*-$B_{12}H_{12}]^{2-}$ dianion (Fig. 1, structure a). This dianion belongs to a point group of I_h symmetry and is considered to be a three-dimensional aromatic system[1]. Such structural architectures are also found in elemental boron itself. Replacement of individual $\{BH\}^{2-}$ vertices in this twelve-vertex polyhedral cluster by various isoelectronic and isolobal[2] main-group element units

doi:10.1135/cccc2010073

leads to a series of icosahedral heteroboranes of lower symmetries than I_h [3]. Introduction of metal vertices into boron hydride clusters is also possible. An archetypical example of such compounds is the cobalt bis(dicarbollide) anion[4], $[3\text{-Co-}(1,2\text{-}C_2B_9H_{11})_2]^-$, called COSAN. Schematically, the COSAN molecule consists of two 12-vertex $\{CoC_2B_9\}$ subclusters that are conjoined by a shared cobalt atom vertex. Extrapolation of this structural principle to a thought experiment that replaces the $\{CoC_2B_9\}$ subunits by two parent $\{B_{12}\}$ moieties would result in the hypothetical $[B_{23}H_{22}]^{5-}$ (Fig. 1, structure b). Both COSAN and $[B_{23}H_{22}]^{5-}$ obey the so-called *mno* rule derived for rationalizing the structures of the macropolyhedral boranes[5]. However, the sharing of a single common vertex is not the only mode of cluster fusion open to the polyhedral boranes. A two-atom edge can be shared, resulting in a mode of condesation seen in, for example, *syn*- and *anti*-$B_{18}H_{22}$ or

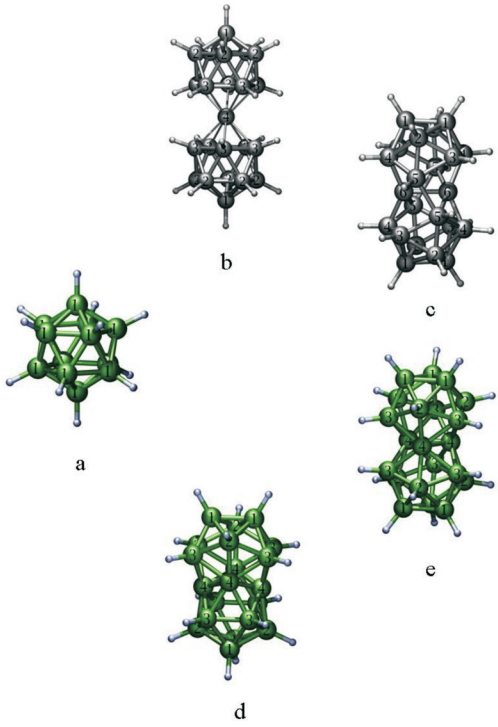

FIG. 1

Molecular models of the dianion $[closo\text{-}B_{12}H_{12}]^{2-}$, **1a**, along with the existing (green) **1d**: $B_{20}H_{16}$, **1e**: $[B_{21}H_{18}]^-$ and hypothetical (black) **1b**: $[B_{23}H_{22}]^{5-}$, **1c**: $[B_{22}H_{20}]^{2-}$ twinned icosahedra. Individual atomic numberings distinguish among nonequivalent types of boron atoms according to symmetries

$[B_{19}H_{22}]^-$ in which two boranyl subclusters are edge-fused[6a,6b]. In our case, conjoining two [*closo*-$B_{12}H_{12}]^{2-}$ clusters via a common B–B edge would result in the hypothetical species, $[B_{22}H_{20}]^{2-}$. (Fig. 1, structure c). Further condensation modes betwen two $\{B_{12}\}$ clusters can be derived from the sharing of a three-vertex triagular face or a four-vertex core of boron atoms. These two possibilities are indeed manifested in experimentally available species and *closo*/*closo* $[B_{21}H_{18}]^-$ (Fig. 1, structure e)[7], *closo*/*closo* $B_{20}H_{16}$ (Fig. 1, structure d), respectively[8–10]. The latter of these compounds was first detected in the 1960's and experimentally shown to have a D_{2d}-symmetrical solid state structure (four kinds of boron atoms), whereas the former species was first synthesized and characterized only recently.

$B_{20}H_{16}$ was prepared for the first time by slow passage of decaborane *nido*-$B_{10}H_{14}$ vapour and H_2 through a discharge between Cu electrodes, and its solid-state structure determined by single-crystal X-ray diffraction[8]. Later an alternative synthetic route to $B_{20}H_{16}$ was proposed based on the catalytic pyrolysis of decaborane at 350 °C [9]. The structure of $B_{20}H_{16}$ in solution was verified using ^{11}B NMR spectroscopy as being consistant with its solid-state structure as determined by X-ray diffraction[8,9]. $[B_{21}H_{18}]^-$, a face-fused diicosahedral borane anion, was prepared from oxidative coupling of two [*closo*-$B_{10}H_{10}]^{2-}$ clusters followed by the insertion of an additional boron-vertex by heating with BH_3NEt_3 [7]. The molecular structure of the salt of $[B_{21}H_{18}]^-$ was elucidated both by a single-crystal X-ray diffraction analysis and ^{11}B NMR spectroscopy[7]. Both characterisation techniques revealed an overall D_{3h} symmetry indicative of four symmetrically-unique boron environments.

In this contribution we present a new synthesis of the macropolyhedral $B_{20}H_{16}$ cluster species and use the ab initio/GIAO/NMR method[3], with a DFT variant, in conjunction with new experimental NMR data to investigate its solution-phase structure and identify its reactive cluster positions.

EXPERIMENTAL

Synthesis

A crude toluene solution of decaborane(14) obtained from the cracking of B_2H_6 in inert atmosphere is evaporated to dryness at 40–50 °C under a partial vacuum generated using a water pump.The precipitated decaborane material is suspended in hexane and this mixture is stirred overnight. The suspension is subsequently filtered and the resulting dark brown hexane filtrate is evaporated to dryness. The crude material is again mixed in hexane and left to stand, during which time decaborane(14) begins to precipitate and crystallise. The remaining hexane solution, removed of the precipitated decaborane(14) via filtration, is evaporated using a water pump and the resulting viscous solution is thence further dried using

an oil pump for a period of ca. two days. The syrup-like residue is then separated by means of partial sublimation. At conditions of 60–90 °C and 1.3 Pa decaborane(14) is collected in an attached cooled receiver, amounting to ca. 60% of the whole mass of processed residue. Subsequent raising of the temperature to 90–105 °C results in the distilling of liquid portions consisting of three isomers of tolyl-decaborane, $CH_3C_6H_4$-$B_{10}H_{13}$. These liquid portions condense into the cooled receiver in an amount ca. 15% of the processed mass. Further temperature elevation to 105–120 °C results in the sublimation and crystallization of $B_{20}H_{16}$, quite unexpectedly, partially contaminated with tolyl-decaboranes. The vitreous residue remaining after completion of sublimation is very likely based on undefined borane polymers. The crude $B_{20}H_{16}$ fraction, including its tolyl-decaborane impurities were dissolved in hot hexane under inert atmosphere and, after partial evaporating of the solvent, white colourless crystals of $B_{20}H_{16}$ appeared on cooling in an yield of 0.1–0.2% with respect to the liquid residue. This unexpected origination of $B_{20}H_{16}$ prompted us to carry out up-to-date NMR measurements along with the computations of the geometry and shielding tensor using well-behaving model chemistries.

NMR Measurements

^{11}B NMR spectroscopical measurements were performed at 11.75 T on a Varian XL-500 instrument in $CDCl_3$.

Computational Details

All calculations were performed with the Gaussian 03 package[11]. Geometry optimizations were started in a symmetry of D_{2d} at the HF/6-31G* level of theory. Frequency computations in the same symmetry gave no imaginary frequency, indicating that this geometry is a true minimum. Final optimizations at RMP2(fc)/6-31G* included the effect of electron correlation.The chemical shieldings were calculated at a DFT level with the GIAO-B3LYP method and utilized a TZP basis set by Huzinaga[12] – (9s5p1d) contracted to [51111,2111,1] for B and 5s1p contracted to [311] for H. It is denoted as IGLO-II, or simply II [13], and is well-established for the calculations of magnetic properties.

RESULTS AND DISCUSSION

During preparation of decaborane(14), *nido*-$B_{10}H_{14}$ by means of the thermal cracking of diborane B_2H_6 in an inert atmosphere, we succeeded in isolating in modest yield the known macropolyhedral cluster, $B_{20}H_{16}$, as a by-product. This new procedure represents the third synthetic route to this species, which is otherwise not easy to make and thus enabled us to study its structure using new ^{11}B NMR spectroscopic measurements including two-dimensional correlated spectroscopy (COSY) experiments (Fig. 2). Table I provides NMR data. There are four signals in the ^{11}B spectrum with an intensity ratio of 4:4:4:8 indicative of the symmetry seen in the solid-state structure of $B_{20}H_{16}$ [8,9]. One peak of intensity four is a singlet in this spectrum and is not split by coupling to any H nucleus (see Table I) and can

therefore be unambiguously assigned to the four naked boron atoms. Assignment of the other resonance peaks to atomic positions are made from comparison of the cross-peaks observed (four possible B–B contacts) in the ^{11}B-^{11}B COSY NMR experiments and the corresponding relative intensities of these resonances.

The final level of the optimization of the molecular geometry of $B_{20}H_{16}$ used the correlated level of theory [MP2(fc)] with 6-31G* basis set and this

TABLE I
The GIAO[a] and experimental $\delta(^{11}B)$ in ppm with respect to $BF_3{\cdot}OEt_2$ and interaction constants (J) in Hz for $B_{20}H_{16}$

No. of B atoms	GIAO	Experimental (data in ref.[8], in CCl_4)	$J(^1H,^{11}B)$
4[b]	3.6	2.6 (3.9)	150
4[c]	10.6	9.6 (11.7)	–
4[d]	–2.2	–4.4 (–4.3)	143
8[e]	–2.4	–6.5 (–4.3)	167

[a] Calculated at the B3LYP level with a TZP basis set by Huzinaga using MP2(fc)/6-31G* geometry, i.e., GIAO-B3LYP/II//MP2(fc)/6-31G*. [b] Boron atoms of two B–B bonds with midpoints that form body diagonal (B1). [c] Naked boron atoms (B4). [d] Two next-next-nearest B···B separations that form with B atoms in [b] two tetraborane cages (B2). [e] The only combination of eight equivalent boron atoms according to symmetry (B4). [f] Originally reported with respect to $B(OCH_3)_3$, recalculated with respect to generally accepted standard $BF_3{\cdot}OEt_2$, $\delta(^{11}B)$ $B(OCH_3)_3$ with respect to the latter was agreed to be 18.1 ppm (ref.[15]).

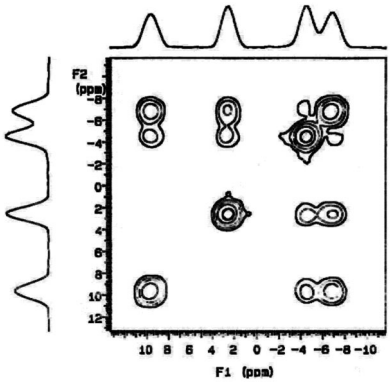

FIG. 2
$^{11}B\{^1H\}$-$^{11}B\{^1H\}$ COSY 2D NMR spectrum of $B_{20}H_{16}$

set of internal coordinates served as an input for computing the corresponding shielding tensor (Table I). As can be seen, four naked boron atoms resonate at a relatively high frequency in relation to other resonances. We can speculate that this might be assigned to the occurrence of paramagnetic contributions to the magnetic shielding constants. Such contributions result from the coupling of suitable occupied and unoccupied molecular orbitals with large coefficients on naked boron atoms. HOMO and LUMO orbitals (Fig. 3) seem to be key for paramagnetic contributions to the shielding tensor of the naked boron atoms since in this part of the molecule the overlap between HOMO and LUMO is visually the most intensive.

There are no unusually long B–B connectivities; all values spanning an interval of ca. 1.75–1.86 Å, B3–B4 being the longest (1.858 Å) and B2–B4 the shortest (1.753 Å). B–B connectivities between the four naked boron atoms, B4–B4, computed at 1.769 Å and the Wiberg bond index[14] for these vectors amounts to 0.52, suggesting that these connectivities are participating in three-center bonding typical for the boranes. A comparison of the experimentally determined and computationally calculated chemical shifts shown in Table I, suggests that the MP2(fc)/6-31G* geometry is a good representation of the actual geometry of $B_{20}H_{16}$ in solution and, in turn, is in a good accord with the solid-state geometry reported in ref.[8], in which B3–B4, B2–B4 and B4–B4 are 1.87, 1.76 and 1.78 Å, respectively. Note that with the exception of B3–B4 there are no significant deviations in bond lengths when comparing the eight remaining different B–B separations in the macropolyhedron with the only one in $[closo\text{-}B_{12}H_{12}]^{2-}$, viz 1.787 Å as computed at MP2/6-31G* within this context.

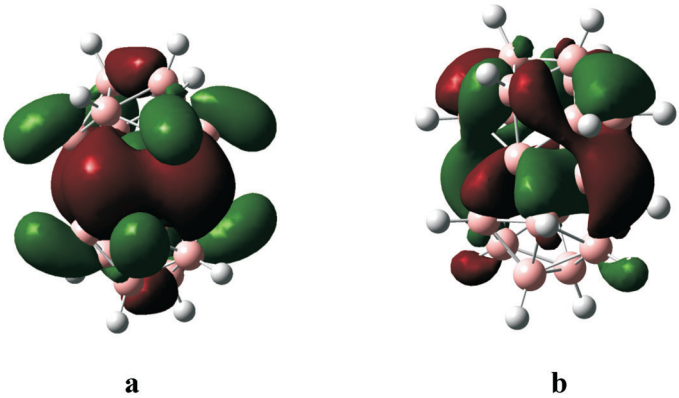

FIG. 3
HOMO (a) and LUMO (b) of $B_{20}H_{16}$ at HF/6-31G*

Despite being known for decades, little is understood of the chemistry of $B_{20}H_{16}$ due to the difficulty of its synthesis. Essentially, the only aspect of its behaviour documented is the ready reactivity of $B_{20}H_{16}$ toward Lewis bases,(e.g. OH^-, OEt^-)[16]. The addition of acetonitrile to $B_{20}H_{16}$ results in the opening of the closed polyhedral structure and the formation of the bis(ligand) adduct $[B_{20}H_{16}(MeCN)_2]$[17]. This adduct is structurally based on a twenty-vertex *closo/nido* arrangement, in which the mode of fusion between the two subclusters of the molecule changes from a shared four-boron core, seen in the parent $B_{20}H_{16}$, to a common triangular face. This structural change is in essence driven by the addition of electrons into the cluster framework from the acetonitrile ligands, a mechanism examined computationally by Jemmis et al.[18] and rationalised in terms of the *mno* rule[18,19]. Coincidentally, our calculations at HF/6-31G* show there to be significant contributions to the LUMO of $B_{20}H_{16}$ from these vertices (see Fig. 3), thus rationalising these cluster sites' propensity to nucleophilic attack. Vector analysis of the experimental dipole moments confirms such an electron-acceptor character of the icosahedral cage itself[20].

Further condensation by four-vertex sharing would lead to a structure of $[B_{28}H_{20}]^{2+}$ (Fig. 4)[19,21], experimental endeavours towards acquiring it would be challenging.

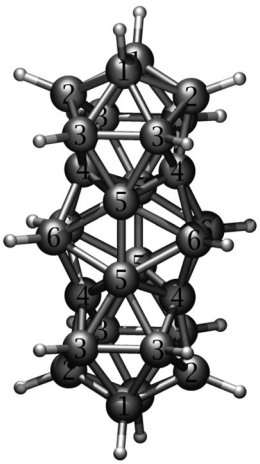

FIG. 4
Molecular model of the hypothetical dication $[B_{28}H_{20}]^{2+}$. Atomic numbering shows nonequivalent types of boron atoms according to symmetry

CONCLUSION

The alternative synthesis of the macropolyhedral borane $B_{20}H_{16}$ has provided the possibility to probe its solution-phase structure using modern NMR spectroscopy supplemented by a computational study that confirm its structure in solution to be analogous to that in the solid-state. Additionally, the computational work here, analysing the contribution of individual boron vertices to cluster HOMO and LUMOs, provides rationale to the experimentally determined sites of nucleophilic attack. With regard to the current interest in the use of neutral macropolyhedral boranes as boron-dopant agents in the fabrication of p-type semiconducting silicon, it is our hope that the synthesis described herein will be of assistance to those attempting to achieve low-energy, shallow implantation.

Financial support of the Czech Science Foundation (Project P208/10/2269) and the Academy of Sciences of the Czech Republic (project M200320904) is greatly appreciated.

REFERENCES

1. Schleyer P. v. R., Najafian K.: *Inorg. Chem.* **1998**, *37*, 3454.
2. Beckett M. A., Croo J. E., Greenwood N. N., Kennedy J. D.: *J. Chem. Soc., Dalton Trans.* **1986**, 1879.
3. See, e.g., Hnyk D., Rankin D. W. H.: *Dalton Trans.* **2009**, 585. The geometries calculated at a correlated level of theory (MP2) are found to be superior both to those derived in terms of a Hartree–Fock scheme and, to some extent, to DFT approaches.
4. For computational study, see Bühl M., Hnyk D., Macháček J.: *Chem. Eur. J.* **2005**, *11*, 4109.
5. a) Jemmis E. D., Balakrisnaranjan M. M., Pancharatna P. D.: *J. Am. Chem. Soc.* **2001**, *123*, 4313; b) Jemmis E. D., Balakrisnaranjan M. M., Pancharatna P. D.: *Chem. Rev.* **2002**, *102*, 93.
6. a) Pitochelli A. R., Hawthorne M. F.: *J. Am. Chem. Soc.* **1962**, *84*, 3218; b) Londesborough M. G. S., Bould J., Baše T., Hnyk D., Bakardjiev M., Holub J., Císařová I., Kennedy J. D.: *Inorg. Chem.* **2010**, *49*, 4092.
7. Bernhardt E., Brauer D. J., Finze M., Willner H.: *Angew. Chem., Int. Ed. Engl.* **2007**, *46*, 2927. ^{11}B NMR spectra were recorded in CD_3CN and we computed $\delta(^{11}B)$ NMR chemical shifts with respect to $BF_3{\cdot}OEt_2$ at GIAO-B3LYP/II//MP2/6-31G* with the following results (in ppm; experimental values from ref.[10] are in brackets): B3, 6.0 (4.7); B2, –18.9 (–18.4); B1, 4.6 (1.9); B4, –23.7 (–20.6).
8. Friedman L. B., Dobrott R. D., Lipscomb W. N: *J. Am. Chem. Soc.* **1963**, *85*, 3505.
9. Miller N. E., Muetterties E. L.: *J. Am. Chem. Soc.* **1963**, *85*, 3506.
10. Alternatively, $B_{20}H_{16}$ can be viewed as a result of sharing two decaboranes (after removing hydrogen bridges and two terminal hydrogens from each moiety) mutually twisted by 90°.

11. Frisch M. J., Trucks G. W., Schlegel H. B., Scuseria G. E., Robb M. A., Cheeseman J. R., Montgomery J. A., Jr., Vreven T., Kudin K. N., Burant J. C., Millam J. M., Iyengar S. S., Tomasi J., Barone V., Mennucci B., Cossi M., Scalmani G., Rega N., Petersson G. A., Nakatsuji H., Hada M., Ehara M., Toyota K., Fukuda R., Hasegawa J., Ishida M., Nakajima T., Honda Y., Kitao O., Nakai H., Klene M., Li X., Knox J. E., Hratchian H. P., Gross J. P., Adamo C., Jaramillo J., Gomperts R., Stratmann R. E., Yazyev O., Austin A. J., Cammi R., Pomelli C., Ochterski J. W., Ayala P. Y., Morokuma K., Voth G. A., Salvador P., Dannenberg J. J., Zakrzewski V. G., Dapprich S., Daniels A. D., Strain M. C., Farkas O., Malick D. K., Rabuck A. D., Raghavachari K., Foresman J. B., Ortiz J. V., Cui Q., Baboul A. G., Clifford S., Cioslowski J., Stefanov B. B., Liu G., Liashenko A., Piskorz P., Komaromi I., Martin R. L., Fox D. J., Keith T., Al-Laham M. A., Peng C. Y., Nanayakkara A., Challacombe M., Gill P. M. W., Johnson B., Chen W., Wong M. W., Gonzalez C., Pople J. A.: *Gaussian 03*, Revision C.02. Gaussian, Inc., Wallingford (CT) 2004.
12. Huzinaga S.: *Approximate Atomic Wave Functions*. University of Alberta, Edmonton 1971. IGLO-II basis sets can be downloaded through http://www.demon-software.com/public_html/download.html
13. Kutzelnigg W., Fleischer U., Schindler M.: *NMR Basic Principles and Progress*, Vol. 23, pp. 165–262. Springer, Berlin 1990.
14. a) Reed A. E., Weinstock R. B., Weinhold F.: *J. Chem. Phys.* **1985**, *83*, 735, and references therein; b) Reed A. E., Weinhold F.: *Chem. Rev.* **1988**, *88*, 899.
15. Heřmánek S.: *Chem. Rev.* **1992**, *92*, 325.
16. Miller N. E., Forstner J. A., Muetterties E. L.: *Inorg. Chem.* **1964**, *3*, 1690.
17. Enemark J., Friedman L. B., Hartsuck J. A., Lipscomb W. N.: *J. Am. Chem. Soc.* **1966**, *88*, 3659.
18. Shameema O., Pathak B., Jemmis E. D.: *Inorg. Chem.* **2008**, *47*, 4375.
19. Balakrishnarajan M. M., Jemmis E. D.: *J. Am. Chem. Soc.* **2000**, *122*, 4516.
20. For charge distribution in 1,2-$C_2B_{10}H_{12}$, see Hnyk D., Všetečka V., Drož L., Exner O.: *Collect. Czech. Chem. Commun.* **2001**, *66*, 1375.
21. Jemmis E. D., Jayasree E. G.: *Acc. Chem. Res.* **2003**, *36*, 816.